A Single Ataxia Telangiectasia Gene with a Product Similar to PI-3 Kinase

Kinneret Savitsky,* Anat Bar-Shira,* Shlomit Gilad, Galit Rotman, Yael Ziv, Lina Vanagaite, Danilo A. Tagle, Sara Smith, Tamar Uziel, Sharon Sfez, Maya Ashkenazi, Iris Pecker, Moshe Frydman, Reli Harnik, Sankhavaram R. Patanjali, Andrew Simmons, Gregory A. Clines, Adam Sartiel, Richard A. Gatti, Luciana Chessa, Ozden Sanal, Martin F. Lavin, N. G. J. Jaspers, A. Malcolm R. Taylor, Colin F. Arlett, Toru Miki, Sherman M. Weissman, Michael Lovett, Francis S. Collins, Yosef Shiloh†

A gene, *ATM*, that is mutated in the autosomal recessive disorder ataxia telangiectasia (AT) was identified by positional cloning on chromosome 11q22-23. AT is characterized by cerebellar degeneration, immunodeficiency, chromosomal instability, cancer predisposition, radiation sensitivity, and cell cycle abnormalities. The disease is genetically heterogeneous, with four complementation groups that have been suspected to represent different genes. *ATM*, which has a transcript of 12 kilobases, was found to be mutated in AT patients from all complementation groups, indicating that it is probably the sole gene responsible for this disorder. A partial *ATM* complementary DNA clone of 5.9 kilobases encoded a putative protein that is similar to several yeast and mammalian phosphatidylinositol-3′ kinases that are involved in mitogenic signal transduction, meiotic recombination, and cell cycle control. The discovery of *ATM* should enhance understanding of AT and related syndromes and may allow the identification of AT heterozygotes, who are at increased risk of cancer.

Ataxia telangiectasia is inherited in a monogenic, autosomal recessive manner, with a worldwide incidence of 1 in 40,000 to 1 in 100,000 (*1*). Ataxia telangiectasia is usually first noticed in toddlers by the appearance of an unsteady gait (ataxia), which reflects cerebellar degeneration and heralds progressive neuromotor deterioration, and the appearance of dilated blood vessels (telangiectases) in the conjunctivae of the eyes and sometimes in the facial skin. Absence or degeneration of the thymus, together with severe deficiencies in the humoral and cellular immune responses, causes recurrent sinopulmonary infections in many patients. Additional symptoms include growth retardation, premature aging, high serum concentrations of α-fetoprotein, chromosomal instability, predisposition to lymphoreticular malignancies, and acute sensitivity to ionizing radiation. Patients usually die during the second or early in the third decade of life.

The pleiotropic nature of the clinical features of AT is manifested also in the cellular phenotype (*2–5*). In addition to chromosomal instability, cells of AT patients have a reduced life-span, higher requirements for serum growth factors, defects in the cytoskeleton, and increased sensitivity to ionizing radiation and radiomimetic chemicals. Inhibition of semiconservative DNA synthesis and cell cycle progression by ionizing irradiation is reduced in AT cells (*6*), suggesting that there are defects in the checkpoints at the G_1 and G_2 phases of the cell cycle (*7*). The increase in stability of p53 after irradiation is significantly delayed in AT cells, which is further evidence of a defective G_1 checkpoint that normally signals the presence of DNA damage (*8*).

Individuals who are heterozygous for AT (~1% of the population) mildly manifest two of the disease characteristics: cancer predisposition and radiation sensitivity. Cancer predisposition in this group has been estimated to be about three- to fourfold that of the general population, with a relative risk for breast cancer in carrier women fivefold that of normal women (*9*). Cellular radiosensitivity is intermediate between that of homozygous patients and unaffected individuals (*10*).

Characterization of heterokaryons has revealed four complementation groups in AT, designated A, C, D, and E (*11*). As it has never been clear whether these complementation groups represent different genes or different mutations within a gene capable of intragenic complementation, researchers have considered the possibility that the disease might be determined by four genes.

A functional cloning approach based on complementation of the cellular phenotype by gene transfer has not identified a gene directly related to the disease (*12–15*). Gatti *et al.* (*16*) applied linkage analysis to locate an AT locus containing the group A mutations on chromosome 11, region q22-23. Subsequently, Ziv *et al.* (*17*) demonstrated linkage to the same region in a group C family. Additional studies indicated that mutations in this region were probably responsible for the majority of AT cases worldwide. In the course of these linkage studies, the location of the AT locus was narrowed to a region of ~3 Mb of DNA (*2, 18*).

We applied further positional cloning steps (*19*) to identify the AT gene or genes in this region. Long-range cloning of the AT locus was performed by constructing a contig of yeast artificial chromosome (YAC) clones across the AT interval and flanking sequences (*20*). This contig made it possible for us to construct a high-density marker map of the region by derivation of microsatellite markers from the YAC clones and by physical localization and ordering of additional markers generated by other laboratories (*21*) (Fig. 1A). This information was used in a consortium-based linkage study of 176 AT families from the United States, England, Turkey, Italy, and Israel (*22*). Individual recombinants in this study placed the AT locus between the markers D11S1818 and D11S1819, whereas the peak of the AT location score was obtained at the marker D11S535, with a two-lod support interval (lod, logarithm of the likelihood ratio for linkage) for AT between D11S1294 and D11S384. The latter interval was estimated at 500 kb (Fig. 1A). No recombinants have been found between AT and markers in this interval. Linkage disequilibrium has also been observed between

K. Savitsky, A. Bar-Shira, S. Gilad, G. Rotman, Y. Ziv, L. Vanagaite, S. Smith, T. Uziel, S. Sfez, M. Ashkenazi, I. Pecker, R. Harnik, A. Sartiel, Y. Shiloh, Department of Human Genetics, Sackler School of Medicine, Tel Aviv University, Tel Aviv 69978, Israel.
D. A. Tagle and F. S. Collins, National Center for Human Genome Research, National Institutes of Health, Bethesda, MD 20892, USA.
M. Frydman, Institute of Human Genetics, Chaim Sheba Medical Center, Tel Hashomer 52621, Israel.
S. R. Patanjali and S. M. Weissman, Boyer Center for Molecular Medicine, Yale University School of Medicine, New Haven, CT 06536–0812, USA.
A. Simmons, G. A. Clines, M. Lovett, Department of Biochemistry and McDermott Center, University of Texas Southwestern Medical Center, Dallas, TX 75235, USA.
R. A. Gatti, Department of Pathology, University of California Los Angeles School of Medicine, Los Angeles, CA 90095, USA.
L. Chessa, Dipartimento di Medicina Sperimentale, Università Degli Studi di Roma "La Sapienza," 00161 Roma, Italy.
O. Sanal, Department of Pediatrics, Faculty of Medicine, Hacettepe University, Ankara, Turkey.
M. F. Lavin, Queensland Institute of Medical Research, Herston, Queensland 4006, Australia.
N. G. J. Jaspers, Department of Cell Biology and Genetics, Erasmus University Rotterdam, 3000 DR Rotterdam, Netherlands.
A. M. R. Taylor, CRC Institute for Cancer Studies, University of Birmingham, Birmingham B15 2TT, UK.
C. F. Arlett, Medical Research Council Cell Mutation Unit, University of Sussex, Falmer, Brighton BN1 9RR, UK.
T. Miki, Laboratory of Cellular and Molecular Biology, National Cancer Institute, Bethesda, MD 20892, USA.

*These authors contributed equally to this work.
†To whom correspondence should be addressed.

AT and markers at the D11S384–D11S1818 region in patients of Moroccan-Jewish and Costa Rican origin (*23*).

Part of the YAC contig spanning the AT interval (*20*) is shown in Fig. 1B. To facilitate identification of transcribed sequences, we also constructed cosmid contigs spanning the D11S384–D11S1818 interval (*24*) (Fig. 1C). Two complementary methods were used for the identification of transcribed sequences: hybrid selection based on direct hybridization of genomic DNA with complementary DNAs (cDNAs) (*25*) and exon amplification, which identifies putative exons in genomic DNA by their splicing capacity (*26*).

In hybrid selection experiments, cosmid and YAC clones served to capture cross-hybridizing sequences in cDNA collections from placenta, thymus, and fetal brain by means of the magnetic bead capture protocol (*27*). YAC clones were bound to a solid matrix and used to select cDNA fragments from a heterogenous cDNA collection representing several human tissues (*28*). The cosmids were also used for exon amplification with the pSPL3 vector (*26*). The captured cDNA fragments and amplified exons were mapped back to the AT region by hybridization to radiation hybrids containing portions of the 11q22-23 region (*29*), and by hybridization to high-density grids containing all the YACs and cosmids spanning this interval. An extensive transcriptional map of the AT region was thus constructed (*30*). Pools of adjacent cDNA fragments and exons, expected to converge into the same transcriptional units, were used to screen cDNA libraries. Figure 1D shows a cluster of five cDNA fragments and three exons that mapped in close proximity to the marker D11S535, where the location score for AT had peaked (*22*). All of these sequences hybridized to the same 5.9-kb cDNA clone, 7-9, obtained from a fibroblast cDNA library (Fig. 1E) (*31*).

Hybridization of the 7-9 cDNA clone to the radiation hybrid panel indicated that the entire transcript was derived from the chromosome 11 locus. The full sequence of this clone was obtained by a shotgun strategy (*32*) and contained 5921 base pairs (bp) which include an open reading frame (ORF) of 5124 nucleotides, a 538-bp 3′ untranslated region, and a 259-bp 5′ sequence containing stop codons in all reading frames (Fig. 1D; GenBank accession number U26455). Genomic sequencing identified the 5′ noncoding region of clone 7-9 as sequences of the adjacent intron. Two other cDNA clones from a leukocyte cDNA library were found to contain this intronic sequence in their 5′ ends. These clones may represent either splicing intermediates or alternatively spliced transcripts of this gene, in which sequences of the adjacent intron were left to serve as an untranslated leader. Alignment of the cDNA with the genomic physical map (Fig. 1, C to E) showed that the corresponding gene is transcribed from centromere to telomere.

Hybridization of a probe containing the entire ORF of clone 7-9 to Northern (RNA) blots from various tissues and cell lines (Fig. 2) revealed a major transcript of 12 kb in all tissues and cell types examined and minor species of various sizes in several tissues, possibly representing alternatively spliced transcripts of the corresponding gene or other similar sequences. Preliminary analysis of additional cDNA clones corresponding to this gene indicated several transcripts generated by alternative splicing combinations. We evaluated the evolutionary conservation of the 7-9 sequence by hybridizing a probe spanning the ORF to a Southern (DNA) blot of samples from a variety of species. Strongly hybridizing bands were observed across most vertebrate species, indicating considerable evolutionary conservation (*33*).

The predicted product of the ORF in cDNA 7-9 is a putative protein of 1708 amino acids, beginning with the first available methionine and ending in a termination codon (Fig. 3). This protein shows considerable similarity to a family of signal transduction mediators involved in controlling the G_1 phase of the eukaryotic cell cycle: the TOR1 and TOR2 proteins in yeast (*34*), as well as their mammalian homologs designated mTOR or RAFT in the rat, and FRAP in humans (*35*) (Fig. 4). The 7-9 putative protein also shows strong similarity to two other yeast proteins: ESR1, an essential yeast protein required for DNA repair and meiotic recombination (*36*) (Fig. 4), and a hypothetical membrane protein of unknown function that was deduced from an ORF (YBL088) identified by sequencing the YB18 locus on chromosome II of *Saccharomyces cerevisiae* (*37*). All of these proteins are 2400 to 2800 amino acid residues

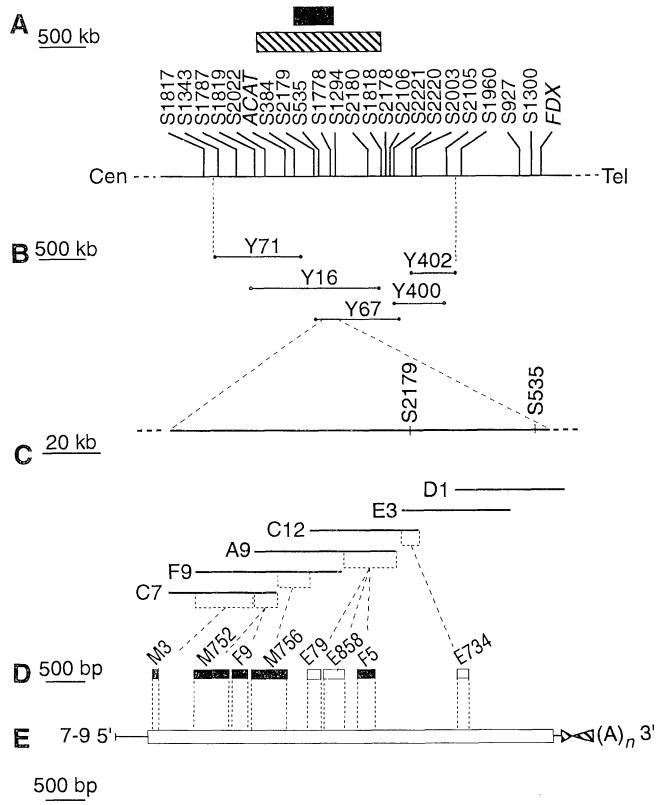

Fig. 1. Positional cloning of the AT candidate gene. (**A**) High-density marker map of the AT region on chromosome 11q22-23 (*21*), constructed by the generation of microsatellite markers within genomic contigs spanning the region and by physical mapping of available markers with the same contigs. To simplify the presentation of the markers, the prefix D11 has been omitted from the marker designations. *FDX*, the adrenal ferredoxin gene; *ACAT*, the acetoacetyl coenzyme A thiolase gene; Cen, centromere; Tel, telomere. The striped box denotes the AT interval, defined recently by individual recombinants between the markers S1818 and S1819 in a consortium linkage study (*22*). The solid box indicates the two-lod support interval for AT obtained in that study, between S1294 and S384. (**B**) Part of a YAC contig constructed across this region (*20*). (**C**) Part of a cosmid contig that spans the S384–S1818 interval, generated by screening a chromosome 11–specific cosmid library with YAC clones Y16 and Y67 and subsequent contig assembly of the cosmid clones by physical mapping (*24*). (**D**) Products of the gene hunting experiments. Solid boxes, cDNA fragments obtained by using cosmid and YAC clones for hybrid selection of cDNAs (*27, 28*) from a variety of tissues; open boxes, putative exons isolated from these cosmids by exon amplification (*26*). These sequences hybridized back to specific cosmids (broken lines), which allowed their physical localization to specific subregions of the contig (dotted frames). (**E**) A 5.9-kb cDNA clone, 7-9, identified in a fibroblast cDNA library (*31*) by using the cDNA fragments and exons in (D) as probes. Dotted lines drawn between the cDNA fragments and exons and the 7-9 cDNA indicate colinearity of sequences. Open box, an open reading frame of 5124 nucleotides; solid lines, untranslated regions; striped arrowheads, two Alu I repetitive elements identified at the 3′ untranslated regions of this clone and 10 smaller clones representing this gene from the same cDNA library and a thymus library.

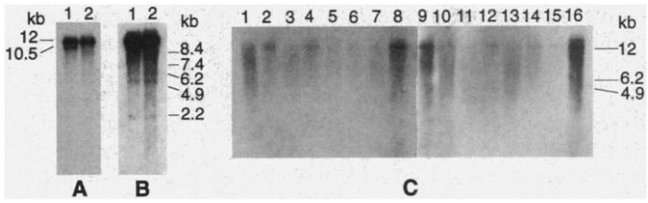


```
   1 MTLHEPANSS ASQSTDLCDF SGDLDPAPNP PHFPSHVIKA TFAYISNCHK
  51 TKLKSILEIL SKSPDSYQKI LLAICEQAAE TNNVYKKHRI LKIYHLFVSL
 101 LLKDIKSGLG GAWAFVLRDV IYTLIHYINQ RPSCIMDVSL RSFSLCCDLL
 151 SQVCQTAVTY CKDALENHLH VIVGTLIPLV YEQVEVQKQV LDLLKYLVID
 201 NKDNENLYIT IKLLDPFPDH VVFKDLRITQ QKIKYSRGPF SLLEEINHFL
 251 SVSVYDALPL TRLEGLKDLR RQLELHKDQM VDIMRASQDN PQDGIMVKLV
 301 VNLLQLSKMA INHTGEKEVL EAVGSCLGEV GPIDFSTIAI QHSKDASYTK
 351 ALKLFEDKEL QWTFIMLTYL NNTLVEDCVK VRSAAVTCLK NILATKTGHS
 401 FWEIYKMTTD PMLAYLQPFR TSRKKFLEVP RFDKENPFEG LDDINLWIPL
 451 SENHDIWIKT LTCAFLDSGG TKCEILQLLK PMCEVKTDFC QTVLPYLIHD
 501 ILLQDTNESW RNLLSTHVQG FFTSCLRHFS QTSRSTTPAN LDSESEHFFR
 551 CCLDKKSQRT MLAVVDYMRR QKRPSSGTIF NDAFWLDLNY LEVAKVAQSC
 601 AAHFTALLYA EIYADKKSMD DQEKRSLAFE EGSQSTTISS LSEKSKEETG
 651 ISLQDLLLEI YRSIGEPDSL YGCGGGKMLQ PITRLRTYEH EAMWGKALVT
 701 YDLETAIPSS TRQAGIIQAL QNLGLCHILS VYLKGLDYEN KDWCPELEEL
 751 HYQAAWRNMQ WDHCTSVSKE VEGTSYHESL YNALQSLRDR EFSTFYESLK
 801 YARVKEVEEM CKRSLESVYS LYPTLSRLQA IGELESIGEL FSRSVTHRQL
 851 SEVYIKWQKH SQLLKDSDFS FQEPIMALRT VILEILMEKE MDNSQRECIK
 901 DILTKHLVEL SILARTFKNT QLPERAIFQI KQYNSVSCGV SEWQLEEAQV
 951 FWAKKEQSLA LSILKQMIKK LDASCAANNP SLKLTYTECL RVCGNWLAET
1001 CLENPAVIMQ TYLEKAVEVA GNYDGESSDE LRNGKMKAFL SLARFSDTQY
1051 QRIENYMKSS EFENKQALLK RAKEEVGLLR EHKIQTNRYT VKVQRELELD
1101 ELALRALKED RKRFLCKAVE NYINCLLSGE EHDMWVFRLC SLWLENSGVS
1151 EVNGMMKRDG MKIPTYKFLP LMYQLAARMG TKMMGGLGFH EVLNNLISRI
1201 SMDHPHHTLF IILALANANR DEFLTKPEVA RRSRITKNVP KQSSQLDEDR
1251 TEAANRIICT IRSRRPQMVR SVEALCDAYI ILANLDATQW KTQRKGINIP
1301 ADQPITKLKN LEDVVVPTME IKVDHTGEYG NLVTIQSFKA EFRLAGGVNL
1351 PKIIDCVGSD GKERRQLVKG RDDLRQDAVM QQVFQMCNTL LQRNTETRKR
1401 KLTICTYKVV PLSQRSGVLE WCTGTVPIGE FLVNNEDGAH KRYRPNDFSA
1451 FQCQKKMMEV QKKSFEEKYE VFMDVCQNFQ PVFRYFCMEK FLDPAIWFEK
1501 RLAYTRSVAT SSIVGYILGL GDRHVQNILI NEQSAELVHI DLGVAFEQGK
1551 ILPTPETVPF RLTRDIVDGM GITGVEGVFR RCCEKTMEVM RNSQETLLTI
1601 VEVLLYDPLF DWTMNPLKAL YLQQRPEDET ELHPTLNADD QECKRNLSDI
1651 DQSFDKVAER VLMRLQEKLK GVEEGTVLSV GGQVNLLIQQ AIDPKNLSRL
1701 FPGWKAWV
```

Fig. 2 (top). Expression of the *ATM* gene. A 5-kb probe spanning the ORF of the 7-9 cDNA was hybridized to RNA blots. (**A**) A blot containing 2 μg of each of lymphoblast and fibroblast polyadenylated RNA in lanes 1 and 2, respectively. A prominent 12-kb band is detected in both tissues, and a minor 10.5-kb species is observed in fibroblasts. (**B**) Longer exposure of the same autoradiogram that shows additional minor bands of various sizes indicating alternatively spliced sequences or other similar sequences. (**C**) The same probe was hybridized against blots containing RNA from 16 human tissues (Clontech, Palo Alto, California). Contents of the lanes (1 to 16) are as follows: 1, pancreas; 2, kidney; 3, skeletal muscle; 4, liver; 5, lung; 6, placenta; 7, brain; 8, heart; 9, spleen; 10, thymus; 11, prostate; 12, testis; 13, ovary; 14, small intestine; 15, colon; and 16, leukocytes. **Fig. 3 (bottom).** Amino acid sequence (*50*) of the deduced translation product encoded by the ORF in cDNA clone 7-9, beginning with the first available methionine residue. The PI-3 kinase signature sequence is underlined.

in length, which could correspond to the product of the 12-kb transcript (Fig. 2).

The similarity between these proteins is greatest across the COOH-terminal 400 amino acids, where identities of 32, 34, and 42% were observed between the 7-9 protein and the TOR proteins, ESR1, and YBL088, respectively (Fig. 4). This region shows high similarity to the lipid kinase domain of the 100-kD catalytic subunit of the signal transduction mediator phosphatidylinositol-3′ kinase (PI-3 kinase) of mammalian cells (*38*), and the corresponding yeast protein Vps34 (*39*) (Fig. 4). A portion of the 7-9 protein (residues 95 to 1080) shows similarity to yet another yeast protein, the *rad3* gene product in the fission yeast *Schizosaccharomyces pombe* (19% identity, 46% similarity; Fig. 4). The rad3 protein is required for the G_2-M cell cycle checkpoint, where it monitors the completion of DNA damage repair and is essential for the correct coupling of mitosis to DNA synthesis. Mutations in this protein in *S. pombe* result in sensitivity to γ- and ultraviolet radiation (*40*).

Southern blot analysis revealed a homozygous deletion in the gene encoding the 7-9 transcript in affected members of family ISAT 9, an extended Palestinian-Arab AT family that has not been assigned to a complementation group. All of the patients in this family are expected to be homozygous by descent for a single AT mutation [see (*41*) for a full pedigree]. The deletion includes almost the entire genomic region spanned by transcript 7-9 and segregates in

Table 1. Mutations identified in the *ATM* gene in AT patients. Abbreviations: aa, amino acid; Compd Htz, compound heterozygote; Del, deletion; Hmz, homozygote; Ins, insertion; ND, not determined; nt, nucleotide; trunc., truncation.

Patient*	Ethnic/geographic origin	Complementation group†	Mutation			Genotype‡
			mRNA sequence change	Predicted protein alteration	Codon	
AT2RO	Arab	A	Del, 11 nt‖	Frameshift, trunc.	499	Hmz
AT3NG	Dutch	A	Del, 3 nt	Del, 1 aa	1512	Compd Htz
AT15LA	Philippine	A	Ins, 1 nt	Frameshift, trunc.	557	Compd Htz
AT3LA§	African American	C	Del, 139 nt, Del, 298 nt¶	Frameshift, trunc.	1196	Compd Htz
AT4LA§	African American	C	Del, 139 nt, Del, 298 nt¶	Frameshift, trunc.	1196	Compd Htz
AT2BR	Celtic/Irish	C	Del, 9 nt‖	Del, 3 aa	1198–1200	Hmz
AT1ABR§	Australian (Irish/British)	E	Del, 9 nt‖	Del, 3 aa	1198–1200	Hmz
AT2ABR§	Australian (Irish/British)	E	Del, 9 nt	Del, 3 aa	1198–1200	Hmz
AT5BI§	Indian/English	D	Del, 6 nt	Del, 2 aa	1079–1080	Compd Htz
AT6BI§	Indian/English	D	Del, 6 nt	Del, 2 aa	1079–1080	Compd Htz
F-2079	Turkish	ND	Ins, 1 nt‖	Frameshift, trunc.	504	Hmz
AT29RM	Italian	ND	Del, 175 nt	Frameshift, trunc.	132	Hmz
AT103LO	Canadian	ND	Ins, 1 nt	Frameshift, trunc.	1635	Hmz
F-596	Palestinian-Arab	ND	Del#	Trunc.	Most of ORF	Hmz

*Cell line designation. AT1ABR and AT29RM are lymphoblastoid cell lines. All other cell lines are primary fibroblasts. †According to Jasper *et al.* (*12*), except for patients AT1ABR and AT2ABR who were typed by Chen *et al.* (*49*). ‡In the compound heterozygotes (Compd Htz), the second mutation is still unidentified. §Sibling patients in both of whom the same mutation was identified. ‖An identical sequence change was observed in genomic DNA. ¶No evidence for deletion was observed in genomic DNA. In both siblings, a normal mRNA was observed in addition to the two deleted species, which may represent abnormal splicing events caused by a splice site mutation. #Reflects a genomic deletion segregating with the disease in family ISAT 9 (Fig. 5).

the family together with the disease (Fig. 5). This finding led to a systematic search for mutations in the 7-9 transcript in additional patients. The restriction endonuclease fingerprinting (REF) method (*42*) was applied to reverse-transcribed and polymerase chain reaction–amplified (RT-PCR) RNA from AT cell lines (*43*). When an abnormal REF pattern was found, the relevant portion of the transcript was directly sequenced (*44*) and another independent RT-PCR product analyzed. In compound heterozygotes, the two alleles were separated by subcloning the RT-PCR products and then individually sequencing them. Genomic sequencing was conducted in some cases to confirm the sequence alteration. Additional family members were studied when available.

Table 1 summarizes sequence alterations found in the 7-9 transcript in 14 AT patients including three sibling pairs. Most of these sequence changes should lead to premature truncation of the protein product, whereas the rest should create in-frame deletions of one to three amino acid residues. Although the consequences of the in-frame deletions remain to be investigated, it is reasonable to assume that they result in impairment of protein function. In one patient, AT3NG, the loss of a serine residue at position 1512 occurs within the PI-3 kinase signature sequence (Fig. 3). This well-conserved domain is distantly related to the catalytic site of protein kinases (*38*). In view of the evidence that mutations in this gene are responsible for AT, it was designated *ATM* (AT mutated).

Additional insight into the function of the *ATM* gene products awaits the complete cloning and sequencing of the rest of the major 12-kb *ATM* transcript and the possible minor transcripts. However, the sequence similarities of *ATM* suggest involvement of the *ATM* gene product in signal transduction, cellular responses to DNA damage, and cell cycle control—the functions defective in AT. The similarity of the ATM protein to PI-3 kinases is of special interest. PI-3 kinase mediates cellular responses to several mitogenic growth factors, to factors triggering cellular differentiation, and to insulin (*38*). Defective protein tyrosine phosphorylation and calcium mobilization in response to the triggering of B cells and T cells support the idea of defects in intracellular signalling pathways in AT (*45*). The role of PI-3 kinase in mediating glucose transport by insulin could be linked to the insulin-resistant diabetes occasionally noticed in AT patients (*1*). PI-3 kinase is required for the prevention of programmed cell death in rat pheochromocytoma cells by nerve growth factor (*46*). This observation may be correlated with the increased nerve cell death in AT and the observation of increased apoptosis in cultured AT cells treated with DNA-damaging agents (*47*).

The TOR proteins are the targets of the immunosuppressant agent rapamycin. In view of the profound immunodeficiency and the defective G_1 checkpoint in AT, it is of interest that the mammalian TOR protein and PI-3 kinase are involved in parallel signal transduction pathways mediating T lymphocyte activation by interleukin-2; both of these pathways end in activation of $pp70^{S6k}$, a protein kinase that is important in the G_1-to-S transition (*48*).

Thus, ATM may be the link between several key physiological processes. The mechanism behind such a link and the pleiotropic nature of AT mutations may be explained by the mosaic structure of this protein, with domains having similarity to other proteins, and by the production of several proteins by alternative splicing.

The convergence of all complementation groups into one gene accords with previous linkage studies that pointed to a single AT locus (*18*, *22*) and suggests that *ATM* is the sole gene responsible for AT. This conclusion requires reconsideration of the complementation group phenomenon that has

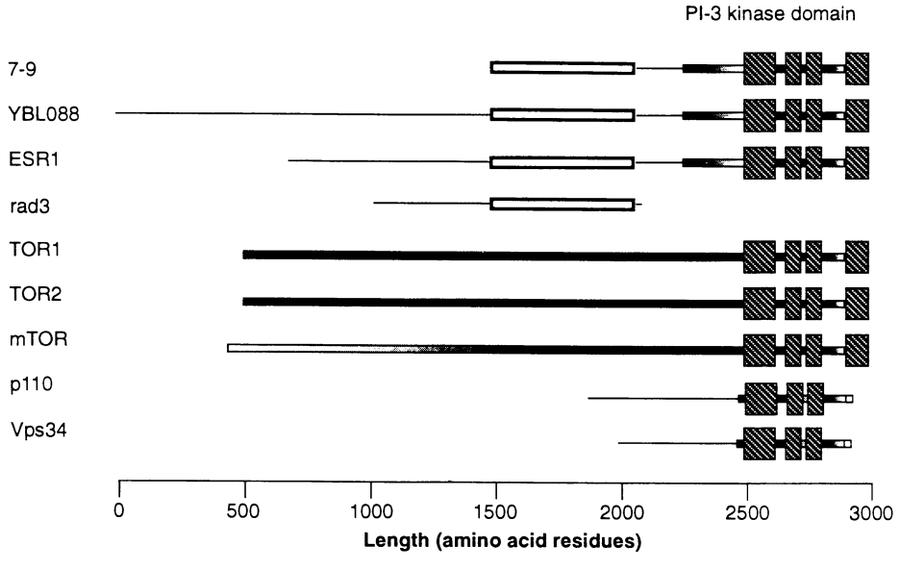

Fig. 4. Schematic diagram of representative PI-3 kinases. The protein sequences indicated were analyzed with the BLAST and MACAW programs (*51*). The sequences were drawn to scale as indicated by the length of the horizontal line for each protein. The 7-9 protein represents a partial sequence. The highly conserved regions within the PI-3 kinase domain are denoted by striped rectangles [Karlin-Altschul probability ($P < 10^{-50}$; 40 to 50% identity]. The white boxes indicate regions of weak similarity with rad3 ($P = 10^{-4}$; 20 to 23% identity). Data (*52*) have shown that the published *rad3* sequence is incomplete and that in fact *rad3* encodes a 2386–amino acid protein with a similar domain structure to the *ESR1* and *TOR* genes. It has recently been shown (*53*) that *ESR1* is identical to a cell cycle checkpoint gene called *MEC1*. *MEC1* mutants in budding yeast have cell cycle and radiosensitivity defects like *rad3* mutants in fission yeast (*54*). Thin lines for each sequence indicate regions with little similarity (<20% identity). TOR1, TOR2, and mTOR share a region of 40 to 67% similarity (thick lines for TOR1 and TOR2; graded lines for mTOR and other proteins indicate a range of similarity) that is not shared by 7-9. p110 is the 110-kD subunit of PI-3 kinase.

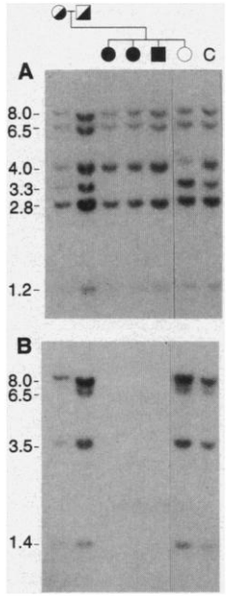

Fig. 5. A deletion in the gene corresponding to the 7-9 transcript in family ISAT 9. (**A**) A probe corresponding to the COOH-terminal 1.2-kb portion of the 7-9 ORF (residues 1311 to 1708, Fig. 3) was hybridized to a Southern blot containing Hind III–digested genomic DNA from several family members [see (*41*) for the complete pedigree]. C, control. (**B**) Hybridization of the same blot with a probe spanning 0.94 kb at the 5′ region of the ORF (residues 360 to 671, Fig. 3) showing complete lack of hybridization with all patient DNAs. Sizes are in kilobases.

dominated AT research for the last 13 years. This is particularly necessary in view of the lack of correlation between complementation group assignment and the mutation sites or nature, and the identical homozygous mutation in patient AT2BR and the sibling patients AT1ABR and AT2ABR previously assigned to two different complementation groups (Table 1). AT patients were assigned to complementation groups on the basis of measurements of radioresistant DNA synthesis (RDS) (*11*) or radiation-induced chromosome breakage (*49*) in heterokaryons. However, RDS and radiosensitivity in AT cells can be dissociated from each other and modulated separately by in vitro manipulations of the cells, in particular by gene transfer (*2*). A variety of cDNAs introduced into AT cells were found to complement the radiometric sensitivity of these cells (*13–15*). Moreover, such complementation was achieved recently by the introduction of cDNA clones of the same gene, the gene for phospholipase A2, into group A cells (*14*) and into group E AT1ABR cells (*15*). Thus, cellular sensitivity and RDS appear to be modulated by genes and physiological factors unrelated to AT. In retrospect, they may have been unsatisfactory experimental clues to the AT genetic defect.

The identification of a single gene responsible for AT should enable clinical geneticists to offer reliable diagnostic tests, including prenatal diagnosis and carrier detection to all AT families. The possible role of the *ATM* gene in cancer predisposition in the general population, particularly breast cancer in women, makes this gene a potential target for screening. Elucidation of the full spectrum of AT mutations may enable the detection of AT carriers in the general population or in specific groups, such as cancer patients or individuals with a positive family history. Carrier detection may also allow a determination of whether preventive measures such as serial mammography are effective or even dangerous in this potentially radiation-sensitive group. Although major ethical and psychological implications of such tests should be considered, these investigations may lead to a better understanding of the genetic background of cancer in humans.

REFERENCES AND NOTES

1. R. P. Sedgwick and E. Boder, in *Handbook of Clinical Neurology*, P. J. Vinken, G. W. Bruyn, H. L. Klawans, Eds. (Elsevier, Amsterdam, 1991), vol. 16, pp. 347–423; R. A. Gatti *et al.*, *Medicine* **70**, 99 (1991).
2. Y. Shiloh, *Eur. J. Hum. Genet.*, in press.
3. A. R. Lehmann, in *Ataxia-Telangiectasia: A Cellular and Molecular Link Between Cancer, Neuropathology and Immune Deficiency*, B. A. Bridges and D. G. Harnden, Eds. (Wiley, Chichester, UK, 1982), pp. 83–102.
4. Y. Shiloh *et al.*, in *Ataxia-Telangiectasia: Genetics Neuropathology and Immunology of a Degenerative Disease of Childhood*, R. A. Gatti and M. Swift, Eds. (Liss, New York, 1985), pp. 111–121.
5. M. F. Lavin, in *Ataxia-Telangiectasia*, vol. H77, *NATO ASI Series*, R. A. Gatti and R. B. Painter, Eds. (Springer-Verlag, Berlin, 1993), pp. 235–255.
6. R. B. Painter and B. R. Young, *Proc. Natl. Acad. Sci. U.S.A.* **77**, 7315 (1980); J. Houldsworth and M. Lavin, *Nucleic Acids Res.* **8**, 3709 (1980).
7. F. Zampetti-Bosseler and D. Scott, *Int. J. Radiat. Biol.* **39**, 547 (1981); M. D. Ford, L. Martin, M. F. Lavin, *Mutat. Res.* **125**, 115 (1984); H. Beamish, K. K. Khanna, M. F. Lavin, *Radiat. Res.* **138**, S130 (1994).
8. M. B. Kastan *et al.*, *Cell* **71**, 587 (1992); K. K. Khanna and M. F. Lavin, *Oncogene* **8**, 3307 (1993).
9. M. Swift *et al.*, *N. Engl. J. Med.* **316**, 1289 (1987); A. L. Borreson *et al.*, *Cancer* **2**, 339 (1990); M. Swift *et al.*, *N. Engl. J. Med.* **325**, 1831 (1991).
10. C. F. Arlett and A. Priestley, in (*4*), pp. 101–109; D. Scott *et al.*, in (*5*), pp. 101–116.
11. J. P. Murnane and R. B. Painter, *Proc. Natl. Acad. Sci. U.S.A.* **79**, 1960 (1982); N. G. J. Jaspers *et al.*, *Cytogenet. Cell Genet.* **49**, 259 (1988).
12. M. H. L. Green *et al.*, *J. Cell Sci. Suppl.* **6**, 127 (1987).
13. M. S. Meyn *et al.*, *Am. J. Hum. Genet.* **53**, 1206 (1993).
14. Y. Ziv *et al.*, *Somatic Cell Mol. Genet.*, in press.
15. P. Chen *et al.*, in preparation.
16. R. A. Gatti *et al.*, *Nature* **336**, 577 (1988).
17. Y. Ziv *et al.*, *Genomics* **9**, 373 (1991).
18. C. M. McConville *et al.*, *Int. J. Radiat. Biol.* **66**, S45 (1994).
19. F. S. Collins, *Nature Genet.* **1**, 3 (1992).
20. G. Rotman *et al.*, *Genomics* **24**, 234 (1994).
21. G. Rotman *et al.*, *Int. J. Radiat. Biol.* **66**, S63 (1994); L. Vanagaite *et al.*, *Hum. Genet.* **95**, 451 (1995).
22. E. Lange *et al.*, *Am. J. Hum. Genet.*, in press.
23. R. Oskato *et al.*, *ibid.* **53**, (suppl.), A1055 (1993); L. Vanagaite *et al.*, unpublished material; N. Uhrhammer *et al.*, *Am. J. Hum. Genet.*, in press.
24. High-density grids were prepared from an arrayed chromosome 11–specific cosmid library and hybridized with ^{32}P-labeled YAC inserts after blocking the probes for 5 hours with Cot-1 and total human DNA. Overlaps between positive cosmids were identified by hybridizing DNA blots with available marker, total cosmid inserts, cosmid ends, or moderately repetitive probes.
25. S. Parimoo *et al.*, *Proc. Natl. Acad. Sci. U.S.A.* **88**, 9623 (1991); M. Lovett *et al.*, *ibid.*, p. 9628.
26. D. M. Church *et al.*, *Nature Genet.* **6**, 98 (1994).
27. J. G. Morgan *et al.*, *Nucleic Acids Res.* **20**, 5173 (1992); D. A. Tagle *et al.*, *Nature* **361**, 751 (product review) (1993).
28. S. Parimoo, R. Kolluri, S. M. Weissman, *Nucleic Acids Res.* **21**, 4422 (1993).
29. C. W. Richard *et al.*, *Genomics* **17**, 1 (1993); M. R. James *et al.*, *Nature Genet.* **8**, 70 (1994).
30. Y. Shiloh *et al.*, *Am. J. Hum. Genet.* **55** (suppl.), A49 (1994).
31. We plated 10^6 plaques of a fibroblast cDNA library in the vector λpCEV29 at a density of 10^6 per 140-mm plate, and replicas were made on nylon filters. The filters were hybridized with ^{32}P-labeled probes, and positive clones were plaque-purified and amplified according to standard techniques.
32. The cDNA inserts were excised from a gel, self-ligated to form concatemers, and sonicated to obtain random fragments. These fragments were size-fractionated by gel electrophoresis, and the 1.0- to 1.5-kb fraction was extracted from the gel and subcloned in a plasmid vector. The end portions of individual clones were sequenced with vector-specific primers in an automated sequencer (Model 373A, Applied Biosystems Division, Perkin-Elmer), and the sequences were aligned with the AutoAssembler program (Applied Biosystems). In the final sequence, each nucleotide position represents at least three independent overlapping readings.
33. Y. Ziv *et al.*, unpublished material.
34. J. Kunz *et al.*, *Cell* **73**, 585 (1993); S. B. Helliwell *et al.*, *Mol. Biol. Cell* **5**, 105 (1994).
35. D. M. Sabatini *et al.*, *Cell* **78**, 35 (1994); E. J. Brown *et al.*, *Nature* **369**, 756 (1994); C. J. Sabers *et al.*, *J. Biol. Chem.* **270**, 815 (1995).
36. R. Kato and H. Ogawa, *Nucleic Acids Res.* **22**, 3104 (1994).
37. Accession no. P38110 in Swissprot database.
38. R. Kapeller and L. C. Cantley, *Bioessays* **16**, 565 (1994); N. Divecha and R. F. Irvine, *Cell* **80**, 269 (1995).
39. P. V. Schu *et al.*, *Science* **260**, 88 (1993).
40. B. L. Seaton *et al.*, *Gene* **119**, 83 (1992); F. Al-Khodairy and A. M. Carr, *EMBO J.* **11**, 1343 (1992); G. Jimenez *et al.*, *Proc. Natl. Acad. Sci. U.S.A.* **89**, 4952 (1992).
41. Y. Ziv *et al.*, *Hum. Genet.* **88**, 619 (1992).
42. Q. Liu and S. S. Sommer, *Biotechniques* **18**, 470 (1995).
43. Total RNA was extracted from cultured cells with the Tri-Reagent system (Molecular Research Center, Cincinnati, OH) and reverse-transcribed with the SuperScript II reverse transcriptase (GibcoBRL, Gaithersburg, MD) and an oligo(dT) primer. The reaction products served as the template for PCR that used gene-specific primers.
44. PCR products were purified with the QIAquick Spin Kit (Qiagen, Hilden, Germany) and dried under vacuum. Primers were added in solution, and the mixture was boiled and snap-frozen in liquid nitrogen. The Sequenase II system (United States Biochemicals, Cleveland, OH) was used to perform the sequencing reactions in the presence of a single-strand binding protein (*T4* gene 32 protein, United States Biochemicals). The reaction products were treated with proteinase K, separated on a 6% polyacrylamide gel, and visualized by autoradiography.
45. M. Lavin *et al.*, unpublished material.
46. R. Yao and G. M. Cooper, *Science* **267**, 2003 (1995).
47. M. S. Meyn, L. Strasfeld, C. Allen, *Am. J. Hum. Genet.* **55**, (suppl.) A3 (1994).
48. D. J. Price *et al.*, *Science* **257**, 973 (1992); M. Monfar *et al.*, *Mol. Cell. Biol.* **15**, 325 (1995).
49. P. Chen *et al.*, *Mutat. Res.* **129**, 165 (1984).
50. Abbreviations for the amino acid residues are A, Ala; C, Cys; D, Asp; E, Glu; F, Phe; G, Gly; H, His; I, Ile; K, Lys; L, Leu; M, Met; N, Asn; P, Pro; Q, Gln; R, Arg; S, Ser; T, Thr; V, Val; W, Trp; and Y, Tyr.
51. G. D. Schuler, S. F. Altschul, D. J. Lipman, *Proteins Struct. Funct.* **9**, 180 (1991).
52. A. M. Carr and N. Bentley, unpublished material.
53. T. Weinert, unpublished material.
54. T. A. Weinert *et al.*, *Genes Dev.* **8**, 652 (1994).

55. This paper is dedicated to the AT patients and their families. We thank the staff of the Department of Human Genetics, Hadassah Hebrew University Medical Center for patient cell lines, D. Lancet and T. Mehlman for sequence analysis, O. Reiner and K. Abel for laboratory protocols and technical guidance, R. Shamir and C. Soderlund for contig alignment programs, S. Sommer and Q. Liu for the REF protocols, M. Boguski for discussions on the MACAW program, A. Chakravarti for discussions on linkage disequilibrium analysis, A. Lehmann, A. Carr, and T. Weinert for unpublished information, B. Amit for technical support, and F. Zetland for manuscript editing. We also wish to acknowledge the contribution of probes and somatic cell hybrid cell lines by C. McConville, M. James, C. Richard, C. Jones, F. Benham and E. Friedberg. The contribution of the chromosome 11–specific cosmid library by L. Deaven, and the experimental help of F. Hisama, T. Sobe, S. Portnoi, C. Spranger, S. King, J. Boals, D. Law, S. C. Chandrasekharappa, C. Robbins, C. Cummings, and L. Pike-Buchanan are gratefully acknowledged. Supported by research grants from the AT Children's Project, The AT Medical Research Foundation, The Thomas Appeal (AT Medical Research Trust), Italian Consiglio Nazionale Ricerche Progetto Finalizzato Applicazioni Cliniche della Ricerca Oncologica (to L.C.), The United States–Israel Binational Science Foundation (to Y.S., D.T. and F.S.C.), the U.S. Department of Energy (grants FG0387 and ERL0548) and the Joseph Drown Foundation (to R.A.G.), the National Center for Human Genome Research (HG00882, to M.L.), and the National Institute of Neurological Disorders and Stroke (NS31763, to Y.S.). This work was carried out in partial fulfillment of the requirements for the Ph.D. degree by K.S. and S.G.

15 May 1995; accepted 30 May 1995